

# ESTIMATING THE DYNAMIC RANGE OF MUSIC SIGNALS VIA RANDOM SUBSAMPLING\*

Pietro Coretto  
Università di Salerno, Italy  
pcoretto@unisa.it

Francesco Giordano  
Università di Salerno, Italy  
giordano@unisa.it

**Abstract.** The dynamic range is an important parameter which measures the spread of sound power. For music signals it is a measure of recording quality. There are various descriptive measures of sound power, none of which has strong statistical foundations. We start from a nonparametric model for sound waves where an additive stochastic term has the role to catch transient energy. The distribution of the variance of the stochastic term is used to measure the dynamic range. The stochastic component accommodates both short range dependence, and long range dependence. This component is recovered by a simple rate-optimal kernel estimator. The distribution of its variance is approximated by a consistent random subsampling method that is able to cope with the massive size of the typical dataset. Based on the latter, we propose a statistic that is able to represent the dynamic range concept consistently.

**Keywords:** music data, dynamic range, nonparametric regression, long range dependence, random subsampling.

**AMS classification:** 97M80 (primary); 62M10, 62G08, 62G09, 60G35 (secondary)

## 1 Introduction

Music signals have a fascinating complex structure with interesting statistical properties. A music signal is the sum of periodic components plus transient components that determine changes from one dynamic level to another. The term “transients” refers to changes in acoustic energy. Transients are of huge interest for several reasons. For technical reasons most recording and listening medium have to somehow compress acoustic energy variations, and this causes that peaks are strongly reduced with respect to average signal level. The latter is also known as “dynamic range compression”. Compression of the dynamic range (DR) increases the perceived loudness. The DR of a signal is the spread of acoustic power. Loss of DR along the recording-to-playback chain translates into a loss

---

\*We thank Bob Katz and Earl Vickers (both members of the Audio Engineering Society) for the precious feedback on some of the idea contained in the paper. The authors gratefully acknowledge support from the University of Salerno grant program “Finanziamento di attrezzature scientifiche e di supporto per i Dipartimenti e i Centri Interdipartimentali - prot. ASSA098434, 2009”.

of audio fidelity. While DR is a well established technical concept, there is no consensus on how to define it and how to measure it, at least in the field of music signals. DR measurement has become an hot topic in the audio business. In 2008 the release of the album “Death Magnetic” (by Metallica), attracted medias’ attention for its extreme and aggressive loud sounding approach caused by massive DR compression. DR manipulations are not reversible, the original dynamic is lost forever (see [Katz, 2007](#); [Vickers, 2010](#), and references therein). Furthermore, there is now consensus that there is a strong correlation between dynamic range and the recording quality perceived by the listener. Practitioners in the audio industry use to measure the DR based on various descriptive statistics for which little is known in terms of their statistical properties ([Boley et al., 2010](#); [Ballou, 2005](#)). In this paper we start from a simple nonparametric model for the signal and we define a measure of DR that can be estimated by a random subsampling method with proven properties both in the context of short range dependence (SRD) and long range dependence (LRD). The idea is that dynamic structure of a music signal is characterized by the energy produced by transient dynamic so that the DR is measured by looking at the distribution of transient power. We propose a nonparametric model composed by two elements: (i) a periodic component consisting in a smooth deterministic function; (ii) a stochastic component representing transients. In this framework transient power is given by the variance of the stochastic component. By consistently estimating the distribution of the variance of the stochastic component, we obtain the distribution of the power expressed by the stochastic component which, in turn, is the basis for constructing our DR statistic.

The idea of decomposing music signals into a deterministic function of time plus a stochastic component is not new (see [Beran, 2004b](#); [Benson, 2006](#), and references therein). However, it is usually assumed that the stochastic term of this decomposition belongs to a class of linear processes. Moreover, according to the  $1/f$ -noise discovery of [Voss and Clarke \(1975\)](#), there is evidence that this process may have a long memory structure. The first novelty in this paper is that we propose a decomposition where the stochastic term can generate both SRD and LRD. Transients with fast vanishing effects (SRD) are assumed to be generated from an  $\alpha$ -mixing process. This allows to accommodate fast vanishing variations beyond those allowed by linear/Gaussian processes. On the other hand transients with slowly decaying effects (LRD) are assumed to be generated by a possibly long-memory autoregressive process. The second contribution of this work is that we develop a rate optimal kernel estimator that works under both SRD and LRD assumptions without any identification of SRD-vs-LRD regime. This improves results in kernel regression literature started with the seminal papers of [Altman \(1990\)](#) (for SRD) and [Hall et al. \(1995\)](#) (for LRD).

Approximation of the distribution of the variance of the stochastic component is done by a subsampling scheme that can cope with both for SRD and LRD. This is developed based on [Politis and Romano \(1994\)](#), [Politis et al. \(2001\)](#) and [Jach et al. \(2012\)](#). The standard subsampling would require to compute the kernel estimate of the deterministic component of the model over the entire sample. The latter is unfeasible given the astronomically large nature of the typical sample size. Hence, a third contribution of the paper is that we propose a consistent random subsampling method that does only require computations subsample-wise. Again, a main advantage of the proposed method is that we do not need to test/select between SRD and LRD. We use the quantiles of the variance distribution of the stochastic component to build our DR statistic. The aim of our DR statistic, is to detect small differences in dynamic levels, and compression. Since DR compression means less audio quality, our DR statistic can be used to measure recording quality, and to com-

pare recordings statistically. The last contribution of the paper is an empirical analysis where we show that: (i) subtle dynamic differences caused by compression are successfully captured by the stochastic component; (ii) the statistical method proposed here provides a consistent DR measure which is easy to interpret in practice.

The paper is organized as follows: in Section 2 we review technical concepts related to physics of sound, in Section 3 we illustrate our modelling strategy, in Section 4 we develop the main statistical tools, in Section 5 we propose our dynamic range statistic, in Section 6 we show empirical results based on real data, finally in Section 7 we set some final remarks. All proofs are collected in the Appendix.

## 2 Background concepts: sound waves, power and dynamic

A sound source radiates acoustic energy and this results in a sound pressure which is captured by the hearing system. Rate of change of acoustic energy is equal to acoustic power, also called sound power. Let  $x(t)$  be a continuous time waveform. At time  $t$  the value  $x(t)$  is equal to the amplitude of an audio stimuli. In general, for a time varying waveform power changes over time. For a continuous waveform  $x(t)$  taking values on the time interval  $T_1 \leq t \leq T_2$ , such that  $\int_{T_1}^{T_2} x(t)dt = 0$ , the power is given by

$$P^{RMS} = C \sqrt{\frac{1}{T_2 - T_1} \int_{T_1}^{T_2} x(t)^2 dt} \quad (1)$$

provided that the integral above exists.  $C$  is an appropriate scaling constant that depends on the measurement unit. Equation (1) defines the so called root mean square (RMS) power. Expression (1) tells us that the power expressed by a waveform is determined by the average magnitude of the wave swings around its average level. In other words the equation (1) reminds us the concept of standard deviation. In acoustics the sound power is conveniently expressed on log-scale because this approximates the psychological and physiological responses of humans to acoustic stimuli (see Ballou, 2005; Crocker, 1998). We conveniently express sound power relatively to a reference value set as baseline obtaining decibels of sound pressure levels,

$$\text{dB}_{\text{SPL}} = 20 \log_{10} \frac{P^{RMS} \text{ Pa}}{20 \mu\text{Pa}},$$

with Pa=Pascal unit. The denominator of  $\text{dB}_{\text{SPL}}$  defines the  $0\text{dB}_{\text{SPL}}$  reference point under which almost no humans can hear. For instance  $40\text{dB}_{\text{SPL}}$  is the sound power produced by a buzzing mosquito around the head,  $180\text{dB}_{\text{SPL}}$  is the sound power produced by a jet engine at one meter.

The sound wave  $x(t)$  can be recorded and stored by means of analog and/or digital processes. In the digital world  $x(t)$  is represented numerically by sampling and quantizing the analog version of  $x(t)$ . The sampling scheme underlying the so called Compact Disc Digital Audio (CDDA), patented by Philips and Sony in the '80s, is called Pulse Code Modulation (PCM). In PCM coding a voltage signal  $x(t)$  is sampled as a sequence of inte-

ger values proportional to the level of  $x(t)$  at equally spaced times  $t_0, t_1, \dots$ . The CDDA is based on PCM coding with sampling frequency equal to 44.1KHz and bit precision equal to 16bits. The sampling frequency at 44.1KHz allows to capture harmonic contents up to 22KHz (by Nyquist theorem), which is slightly above the upper limit of the human hearing system. The 16bits precision means that the signal  $x(t)$  is quantized using  $2^{16}$  integer values. The quantization process introduces rounding errors also known as quantization noise, or quantization error (see [Bennett, 1948](#); [Perez-Alcazar and Santos, 2002](#)). Each operation in the PCM domain increases the energy of the quantization noise, which is considered as the main source of digital noise. Based on the PCM samples  $\{x_0, x_2, \dots, x_T\}$ , and under strong conditions on the structure of the underlying  $x(t)$ , the RMS power can be approximated by

$$P_T^{RMS} = \sqrt{\frac{1}{T+1} \sum_{t=0}^T x_t^2}. \quad (2)$$

$P_T^{RMS}$  is the sample analog of (1), provided that the average of sample values is approximately equal to zero (which is always the case for music signals). Given a reference waveform one can construct a PCM analog of  $\text{dB}_{\text{SPL}}$  by defining ‘‘Full Scale Decibels’’

$$\text{dBFS} = 20 \log_{10} \frac{P_T^{RMS}}{P_0}, \quad (3)$$

where  $P_0$  is the RMS power of a reference waveform such that its power doesn’t depend on  $T$ , and its range covers the range of PCM quantization levels. Usually the reference waveform is either set to a sine wave or a square wave. If the PCM samples are scaled onto the interval  $[-1,1]$ ,  $P_0 = 1/\sqrt{2}$  with reference to a sine wave, and  $P_0 = 1$  with reference to a square wave. For the sake of simplifying calculations we set  $P_0 = 1$  in this paper, even though  $1/\sqrt{2}$  is more popular. dBFS is commonly considered as DR measure because it measures the spread between average sound power and the peak power of a reference signal.

Notice that the dBFS definition above depends on  $T$  because of  $P_T^{RMS}$ . For most real-world signal power changes strongly over time. In [Figure 1](#) we report a piece of sound extracted from the left channel of the song ‘‘In the Flesh?’’ by Pink Floyd. The song starts with a soft sweet lullaby corresponding to Block 1 magnified in the bottom plot. However, at circa 20.39s the band abruptly starts a sequence of blasting riffs. The wave reported in [Figure 1](#) takes one second of music centered around the previous time point. If we would look at the plot with statistics in mind, we would say that we have a time series with a tremendous structural break, there are two regimes with completely different dynamic structures. But the sample reported is only a tiny fraction of the entire song, and if we would look at the entire wave we would have seen several of such breaks and changes. We learn two things: (i) sound power of music signals can change tremendously over time; (ii) the sound power we measure depends on  $T$ , that is the time horizon on which we integrate the squared magnitude of the signal.

In the audio engineering community the practical approach is to time-window the signal and compute average power across windows, then several forms of DR statistics are computed (see [Ballou, 2005](#)) based on dBFS. In practice one chooses a  $T$ , then splits the PCM sequence into blocks of  $T$  samples allowing a certain number  $n_o$  of overlapping samples between blocks, let  $\overline{P_T^{RMS}}$  be the average of  $P_T^{RMS}$  values computed on each block, finally

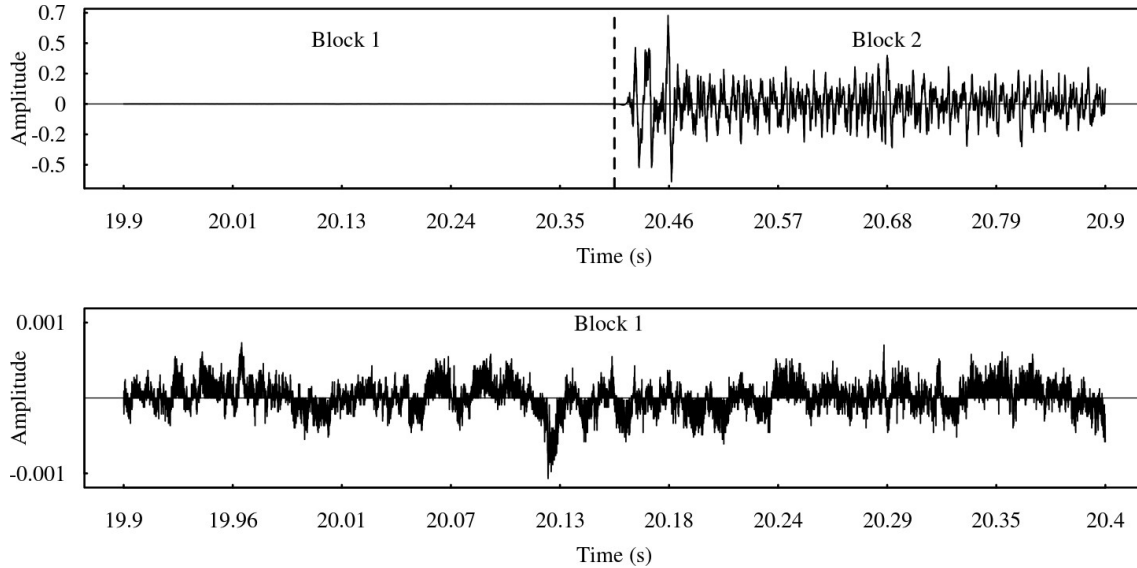


Figure 1: Waveform extracted from the left channel of the song “*In the Flesh?*” from “*The Wall*” album by Pink Floyd (Mobile Fidelity Sound Lab remaster, catalog no. UDCD 2-537). Top plot captures 980ms of music centered at time 20.39524s (vertical dashed line). Bottom plot magnifies Block 1.

a simple DR measure, that we call “sequential DR”, is computed as

$$\text{DRS} = -20 \log_{10} \frac{\overline{P^{RMS}_T}}{x_{\text{peak}}}, \quad (4)$$

where  $x_{\text{peak}}$  is the observed maximum absolute value. The role of  $x_{\text{peak}}$  is to scale the DR measure so that it does not depend on the range of PCM values covered by the recorded signal.  $\text{DRS}=10$  means that on average the RMS power is 10dBFS below the maximum signal amplitude. Even though DRS numbers are easily interpretable, the statistical foundation is weak. Since the blocks are sequential,  $T$  and  $n_o$  determine the blocks uniquely regardless the structure of the signal at hand. For music signals, a common default value is a block length of 50ms with 25% to 50% of overlapping samples. This is because 50ms will contain an entire cycle of the lowest frequency detectable by the average human hearing (that is 20Hz). [Boley et al. \(2010\)](#) reports various qualitative justifications and recommendations for various window lengths based on physical arguments. To our knowledge there is no literature that systematically investigates the effects of windows type and length for real world music signals. In the case of Figure 1 what happens if  $T, n_o$  are picked so that a power measurement is taken in the middle of the transition? The second issue is whether the average  $\overline{P^{RMS}_T}$  is a good measure of the sound power distribution to express the DR concept. Certainly the descriptive nature of the DRS statistic, and the lack of a stochastic framework, does not allow to make inference and judge numbers consistently.

### 3 Statistical aspects of sound waves and modelling

The German theoretical physicist Herman Von Helmholtz (1885) discovered that within small time intervals sound signals produced by instruments are periodic and hence rep-

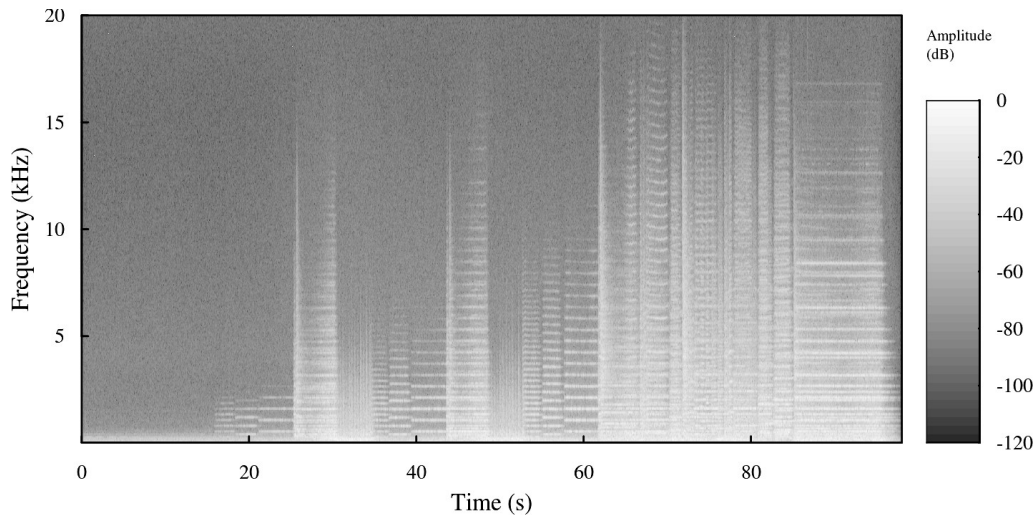


Figure 2: Spectrogram of the right channel of the opening fanfare of “Also Sprach Zarathustra” (Op. 30) by Richard Strauss, performed by Vienna Philharmonic Orchestra conducted by Herbert von Karajan (Decca, 1959). The power spectra values are expressed in dBFS scale and coded as colors ranging from black (low energy) to white (high energy).

representable as sums of periodic functions of time. The latter implies a discrete power spectrum. [Risset and Mathews \(1969\)](#) studies the local behavior of the harmonic components of sound signals from instruments playing simple tunes. They discovered that the intensity of the harmonic components varied strongly over time even for short time lengths. They also showed how in reality instruments have a spectral energy distribution that is not discrete. [Irizarry \(2001\)](#) presents examples of time windowed spectrogram for single tunes of acoustic instruments. He shows that, even though locally the signals are approximately periodic, the harmonic components are time-varying. Figure 2 reports the spectrogram of a famous fanfare expressed in dBFS. This is a particularly dynamic piece of sound. The orchestra plays a soft opening followed by a series of transients at full blast with varying decay-time. There are several changes in the spectral distribution over time. At particular time points there are peaks localized in several frequency bands, but there is a continuum of energy spread between peaks. Figure 2 shows that while the periodic component is strong, there is a relevant continuous component. Several transients change the acoustic energy sharply, and during those transients the energy is spread continuously over a wide frequency bandwidth. The latter supports that idea that transient changes are strongly characterized by continuous spectral components.

In their pioneering works [Voss and Clarke \(1978, 1975\)](#) found evidence that, at least for some musical instruments, once the recorded signal is passed through a low-pass filter, its power spectrum resembles  $1/f$ -noise or similar fractal processes.  $1/f$ -noise is a stochastic process where the spectral density follows the power law  $c|f|^{-\gamma}$ , where  $f$  is the frequency,  $\gamma$  is the exponent, and  $c$  is a scaling constant.  $\gamma = 1$  gives pink noise, that is just an example of such processes. [Brillinger and Irizarry \(1998\)](#) and [Beran \(2004a\)](#) found similar evidence. It seems that in many occasions a music signal has a spectrum approximately following the previous law with  $\gamma$  near one. A nearly unitary value of  $\gamma$  implies long-memory, in fact, that means that a large proportion of the variance is explained by low-frequency components. [Beran \(2004b\)](#) discusses the use of long-memory autoregressive processes (ARFIMA) to capture this behaviour. Whether the  $1/f$ -noise feature is a struc-



tural component of a music signals is yet to be demonstrated. As explained in Brillinger and Irizarry (1998), the empirical evidence is based on spectral methods acting as if the processes involved were stationary, but this is often not the case in practice. Moreover, Brillinger and Irizarry (1998) found evidence of departure of the stochastic component from linearity and Gaussianity. Departure from linearity/Gaussianity is connected with SRD rather than LRD. Our empirical experience confirmed that in most cases, within the same song, one can find all these effects (see example of Figure 3 and discussion in Section 4.1). Therefore, we need a statistical model that is general and rich enough to accommodate both SRD and LRD.

These observations are essential to motivate the following model for the PCM samples. Let  $\{Y_t\}_{t \in \mathbb{Z}}$  be a sequence such that

$$Y_t = s(t) + \varepsilon_t, \quad (5)$$

where  $s(\cdot)$  is a real valued smooth function of time, and  $\{\varepsilon_t\}_{t \in \mathbb{Z}}$  is a real valued stochastic process. It is important to notice that (5) is by no means interpretable as a Tukey-kind signal plus noise decomposition often adopted in signal analysis. Here  $\{\varepsilon_t\}_{t \in \mathbb{Z}}$  is a structural component responsible for the continuous part of the power spectrum. Since the sampling rate is fixed (e.g. 44KHz) we can assume that the autocorrelations of  $\{\varepsilon_t\}$ , denoted by  $\rho(k)$  for  $k = 1, 2, \dots$ , do not depend on the length of time series. The observable (recorded) sound wave  $Y_t$  deviates from  $s(t)$  because of several factors: (i) presence of non-harmonic components; (ii) transient changes in acoustic energy; (iii) several sources of noise injected in the recording path. We call the process  $\{\varepsilon_t\}_{t \in \mathbb{Z}}$  the “stochastic sound wave” (SSW). The role of the variance of the SSW is crucial in this paper because it is used to construct the DR measure.

**Remark 1.** Imagine we have a device that reduces large energy swings. In signal processing such a device is called “dynamic compressor”. A compressor reduces the peakness of the sound energy especially at transients. Hence measuring the power of the transient component should reveal dynamic variations better than if we would look at observed samples. It turns out that the power of the transient component in our model coincides with the variance of  $\varepsilon_t$ . The latter is time varying, and the proposed DR measure is based on its distribution.

The model is completed by the following assumptions.

**A1.** *The function  $s(t)$  has a continuous second derivative,  $t$  takes equally spaced values in  $(0, 1)$ .*

Assumption **A1** imposes a certain degree of smoothness for  $s(t)$ . This is because we want that the stochastic term absorbs transients while  $s(t)$  mainly models long-term periodic behaviours. We assume that the sequence  $\{\varepsilon_t\}_{t \in \mathbb{Z}}$  belongs to a fairly rich class of stochastic processes able to accommodate SRD and LRD:

**A2.** *The SSW fulfils one of the following:*

(SRD)  $\{\varepsilon_t\}_{t \in \mathbb{Z}}$  is a strictly stationary and  $\alpha$ -mixing process with mixing coefficients  $\alpha(k)$ ,  $\mathbb{E}[\varepsilon_t] = 0$ ,  $\mathbb{E}|\varepsilon_t^2|^{2+\delta} < +\infty$ , and  $\sum_{k=1}^{+\infty} \alpha^{\delta/(2+\delta)}(k) < \infty$  for some  $\delta > 0$ .

(LRD)  $\varepsilon_t = \sum_{j=0}^{\infty} \psi_j a_{t-j}$  with  $\mathbb{E}[a_t] = 0$ ,  $\mathbb{E}[a_t^4] < \infty \quad \forall t$ ,  $\{a_t\} \sim i.i.d.$ ,  $\psi_j \sim C_1 j^{-\beta}$  with  $\beta = \frac{1}{2}(1 + \gamma_1)$ ,  $C_1 > 0$  and  $1/5 < \gamma_1 \leq 1$ .

SRD is a rather general  $\alpha$ -mixing assumption. It allows to overcome the usual linear process assumption which is essential to model fast decaying energy variations. Serial dependence is allowed by **A2**-SRD, but this dependence vanishes at some point. Existence of the fourth moment is not that strong in practice, because it implies finite power variations, which is something that has to hold otherwise recording would be impossible. **A2**-LRD has the role to capture situations where the continuous part of the spectrum introduces long-range dependence. The LRD is controlled by  $\gamma_1$  approaching to 1. **A2**-LRD assumes a linear structure while **A2**-SRD does not. As previously noted, this is because LRD effects are more common to appear with a linear autoregressive structure. Moreover, **A2**-LRD is compatible with the classical parametric models for LRD, e.g. the well known ARFIMA class, already used to capture the  $1/f$ -noise phenomenon. It is important to stress that we are not interested in identifying SRD-vs-LRD, and we want to avoid the additional estimation of the LRD order. The latter is crucial in most parametric models for LRD. Assumption **A2** only defines plausible stochastic structures that can coexist within distinct fragments of the same complex music signals. Within the structures delimited by **A2**, we will show consistency of the smoothing-subsampling method developed in the next section.

## 4 Estimation

### 4.1 Smoothing

Estimation of  $s(t)$  is performed based on the classical Priestley-Chao kernel estimator (Priestley and Chao, 1972)

$$\hat{s}(t) = \frac{1}{nh} \sum_{i=1}^n K\left(\frac{t - i/n}{h}\right) y_i, \quad (6)$$

under the following assumption

**A3.**  $K(\cdot)$  is a density function with compact support and symmetric about 0. Moreover,  $K(\cdot)$  is Lipschitz continuous of some order. The bandwidth  $h \in H = [c_1 \Lambda_n^{-1/5}; c_2 \Lambda_n^{-1/5}]$ , where  $c_1$  and  $c_2$  are two positive constants such that:  $c_1$  is arbitrarily small,  $c_2$  is arbitrarily large, and

$$\Lambda_n := \begin{cases} n & \text{if } \mathbf{A2-SRD} \text{ holds,} \\ \frac{n}{\log n} & \text{if } \mathbf{A2-LRD} \text{ holds with } \gamma_1 = 1, \\ n^{\gamma_1} & \text{if } \mathbf{A2-LRD} \text{ holds with } 1/5 < \gamma_1 < 1. \end{cases} \quad (7)$$

Whenever  $n \rightarrow \infty$  it happens that  $h \rightarrow 0$  and  $\Lambda_n h \rightarrow \infty$ .

Without loss of generality we will use the Epanechnikov kernel for its well known efficiency properties, but any other kernel function fulfilling **A3** is welcome. Altman (1990) introduces the kernel regression problem with dependent additive errors, and shows that under serial correlation standard bandwidth optimality theory no longer applies. The author proposes an optimal bandwidth estimator based on cross-validation to which this work is inspired. However, Altman's theory does not apply here for three reasons: (i) we allow for LRD; (ii) in this paper  $\{\varepsilon_t\}_{t \in \mathbb{Z}}$  is not restricted to the class of linear processes unless the dependence is of LRD-type; (iii) we work based on sampling correlations rather than



assuming that the autocorrelation function is known. Let  $\hat{\varepsilon}_t = y_t - \hat{s}(t)$ , and let us define the cross-validation function

$$\text{CV}(h) = \left[ 1 - \frac{1}{nh} \sum_{j=-M}^M K\left(\frac{j}{nh}\right) \hat{\rho}(j) \right]^{-2} \frac{1}{n} \sum_{i=1}^n \hat{\varepsilon}_i^2, \quad (8)$$

where the first term is the correction factor à la Altman, with the difference that it depends on the estimated autocorrelations of  $\{\varepsilon_t\}_{t \in \mathbb{Z}}$  up to the  $M$ th order. Notice that Altman's contribution does not deal with the choice of the smoothing parameter  $M$ . Intuitively consistency of the bandwidth selector can only be achieved if  $M$  increases at a rate smaller than  $nh$ . In our proposal  $M$  is chosen so that the following technical assumption holds.

**A4.** *Whenever  $n \rightarrow \infty$ ; then  $M \rightarrow \infty$  and  $M = O(\sqrt{nh})$ .*

The previous condition makes clear the relative order of the two smoothing parameters  $M$  and  $h$ . The bandwidth is estimated by minimizing the cross-validation function, that is

$$\hat{h} = \operatorname{argmin}_{h \in H} \text{CV}(h)$$

Let  $\text{MISE}(h; \hat{s})$  be the mean integrated square error of  $\hat{s}(\cdot)$ , and let  $h^*$  be the global minimizer of  $\text{MISE}(h; \hat{s})$ .

**Proposition 1.** *Assume [A1](#), [A2](#), [A3](#) and [A4](#).  $\hat{h}/h^* \xrightarrow{p} 1$  as  $n \rightarrow \infty$ .*

Proof of Proposition 1 is given in the Appendix. The previous statement relates  $\hat{h}$  to the optimal global bandwidth for which convergence rate is known, that is  $O(\Lambda_n^{-1/5})$ . The importance of allowing both SRD and LRD is shown in Figure 3, where we report windowed periodogram spectral density estimates of  $\{\varepsilon_t\}_{t \in \mathbb{Z}}$  obtained from two subsamples of the top wave of Figure 1. The SSW has been estimated based on (6) and (8) on subsamples of length equal to 50ms. The first subsample has been randomly chosen within Block 1 of Figure 1, while the second has been randomly chosen within Block 2. Discrete-time Fourier transform measurements have been widowed using Hanning window. Points in the plots correspond to spectral estimates at FFT frequencies scaled to dBFS (log-scale). It can be seen that the two spectrum show dramatic differences. In the first one the energy spread by the SSW is modest and near the shape and level of uncorrelated quantization noise. The rhs spectrum shows a pattern that suggests the presence of LRD. In fact, except the behaviour in the 500Hz–4KHz frequency range, the steep linear shape of the spectrum on log-log coordinates reminds approximately the shape of the  $1/f$ -noise spectrum. We note here that, particularly in the 20Hz–4KHz frequency range, the rhs spectrum shows that the SSW spreads a lot of energy. The latter confirms the idea that there are music sequences where the SSW in (5) cannot be seen as the usual “error term”. In the end, it is remarkable that these extremely diverse stochastic structures coexist within just one second of music.

**Remark 2.** The previous result improves the existing literature in several aspects. First of all, the proposed framework leads to a kernel regression estimator that is optimal under both SRD and LRD. The key feature of the smoothing method proposed here is that one does not need to identify the type of dependence (i.e. SRD vs LRD). There are only two smoothing tunings:  $h$  is estimated optimally, and  $M$  is fixed according to [A4](#). Regarding SRD one needs to compare to [Altman \(1990, 1993\)](#), [Hart \(1991\)](#), [Xia and Li \(2002\)](#) and

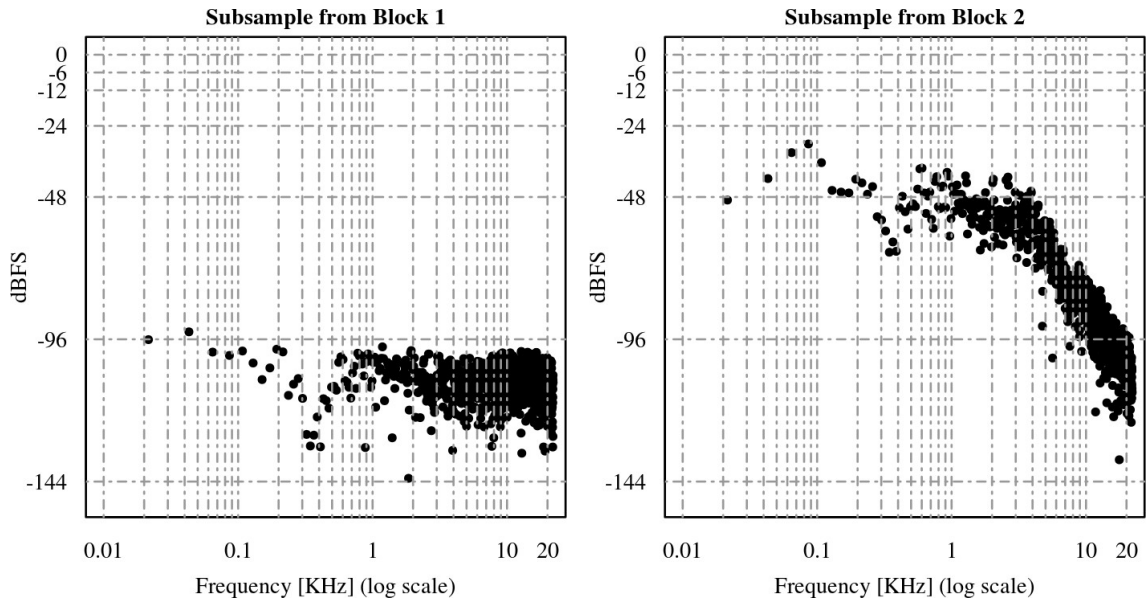


Figure 3: Windowed periodogram power spectral density estimates of the SSW obtained in two subsamples of size 50ms extracted from the wave reported in Figure 1. Plot on the rhs refers to a subsample randomly chosen within “Block 1”, while the plot on the lhs refers to a subsample randomly chosen within “Block 2”.

Francisco-Fernández et al. (2004). The improvement in this case is that: (i) we are able to overcome the linearity/gaussianity of  $\{\varepsilon_t\}_{t \in \mathbb{Z}}$  without assumptions on high-order and mixed moments; (ii) we give a clear indication of how the tuning parameter in the cross-validation function should be set, that is take  $M = \lfloor \sqrt{nh} \rfloor$ . The latter has not been addressed in the literature before, but the choice of  $M$  is crucial. Regarding LRD, here the result of Proposition 1 should be compared to Hall et al. (1995). Compared to the latter: (i) we simplify the methodology eliminating the smoothing parameter to deal with LRD, that is the length of blocks for the leave- $k$ -out cross-validation (see Section 2.3 Hall et al., 1995). This is because  $\text{CV}(\cdot)$  already incorporates the dependence structure, and  $M$  is able to correct (8) without any step where one identifies whether LRD or SRD applies; (ii) we don’t assume existence of high-order moments of  $\{\varepsilon_t\}_{t \in \mathbb{Z}}$ .

## 4.2 Random Subsampling

In analogy with equation (2), RMS power of the SSW is given by the sampling standard deviation of  $\{\varepsilon_t\}_{t \in \mathbb{Z}}$ . Equation (2) only takes into account sum of squares, this is because theoretically PCM are always scaled to have zero mean. Notice that, even though we assume that  $\{\varepsilon_t\}_{t \in \mathbb{Z}}$  has zero expectation, we define RMS based on variances taking into account the fact that quantization could introduce an average offset in the PCM samples. Let us introduce the following quantities:

$$V_n = \frac{1}{n} \sum_{i=1}^n (\varepsilon_i - \bar{\varepsilon})^2, \quad \text{with} \quad \bar{\varepsilon} = \frac{1}{n} \sum_{i=1}^n \varepsilon_i. \quad (9)$$

Define

$$\tau_n := \begin{cases} n^{1/2} & \text{if **A2**-SRD holds,} \\ n^{1/2} & \text{if **A2**-LRD holds with } 1/2 < \gamma_1 \leq 1, \\ \left(\frac{n}{\log n}\right)^{1/2} & \text{if **A2**-LRD holds with } \gamma_1 = 1/2, \\ n^{\gamma_1} & \text{if **A2**-LRD holds with } 1/5 < \gamma_1 < 1/2. \end{cases} \quad (10)$$

Although the sequence  $\{\varepsilon_t\}_{t \in \mathbb{Z}}$  is not observable, one can approximate the power distribution using its estimate. Replacing  $\varepsilon_i$  with  $\hat{\varepsilon}_i$  in the previous formula we obtain:

$$\hat{V}_n = \frac{1}{n} \sum_{i=1}^n (\hat{\varepsilon}_i - \bar{\hat{\varepsilon}})^2, \quad \text{with } \bar{\hat{\varepsilon}} = \frac{1}{n} \sum_{i=1}^n \hat{\varepsilon}_i.$$

The distribution of  $\hat{V}_n$  can now be used to approximate the distribution of  $V_n$ . One way to do this is to implement a subsampling scheme à la [Politis et al. \(2001\)](#). That is, for all blocks of observations of length  $b$  (subsample size) compute  $\hat{V}_n$ . This means that there would be  $n - b + 1$  subsamples to explore. Then one hopes that the empirical distribution of the  $n - b + 1$  subsample estimates of  $\hat{V}_n$  agrees with the distribution of  $V_n$  when both  $n$  and  $b$  grow large enough at a certain relative speed. This is essentially the subsampling scheme proposed by [Politis et al. \(2001\)](#), but it is of limited practical use here. A three minutes stereo song contains  $n = 15,876,000$  samples, which means that one has to compute  $\hat{s}(t)$  on such a long series. Even if this is in principle possible it would require a large computational power hardly achievable by regular computers. We solve the problem by introducing a variant to the subsampling scheme previously described. Namely, instead of estimating  $s(t)$  on the entire series, we estimate it on each subsample separately, then we use the average estimated error computed block-wise instead of the whole sample. Moreover, a block-wise kernel estimate of  $s(t)$  allows to work with the simpler global bandwidth instead of the more complex local bandwidth without losing too much in the smoothing step.

At a given time point  $t$  we consider a block of observations of length  $b$ , and we consider the following statistics

$$V_{n,b,t} = \frac{1}{b} \sum_{i=t}^{t+b-1} (\varepsilon_i - \bar{\varepsilon}_{b,t})^2, \quad \text{and} \quad \hat{V}_{n,b,t} = \frac{1}{b} \sum_{i=t}^{t+b-1} (\hat{\varepsilon}_i - \bar{\hat{\varepsilon}}_{b,t})^2,$$

with  $\bar{\varepsilon}_{b,t} = b^{-1} \sum_{i=t}^{t+b-1} \varepsilon_i$  and  $\bar{\hat{\varepsilon}}_{b,t} = b^{-1} \sum_{i=t}^{t+b-1} \hat{\varepsilon}_i$ . The empirical distribution functions of  $V_{n,b,t}$  and  $\hat{V}_{n,b,t}$  will be computed as

$$G_{n,b}(x) = \frac{1}{n-b+1} \sum_{t=1}^{n-b+1} \mathbb{1} \{ \tau_b(V_{n,b,t} - V_n) \leq x \},$$

$$\hat{G}_{n,b}(x) = \frac{1}{n-b+1} \sum_{t=1}^{n-b+1} \mathbb{1} \left\{ \tau_b(\hat{V}_{n,b,t} - V_n) \leq x \right\}.$$

$\mathbb{1}\{A\}$  denotes the usual indicator function of the set  $A$ .  $\tau_b$  is defined in (10). Lemma 2 and 3 in the Appendix state that the subsampling based on statistic (9) is consistent under both **A2**-SRD and **A2**-LRD. Notice that results in [Politis et al. \(2001\)](#) can only be used to deal with SRD. The LRD treatment is inspired to [Hall et al. \(1998\)](#) and [Jach](#)

et al. (2012). However we improve upon their results in the sense that the Gaussianity assumption for  $\varepsilon_t$  is avoided under **A2**-LRD with  $1/2 < \gamma_1 \leq 1$ . The quantiles of the subsampling distribution also converges to the quantiles of  $V_n$ . This is a consequence of the fact that  $\tau_n V_n$  converges weakly (see Remark 5). Define the empirical distributions:

$$F_{n,b}(x) = \frac{1}{n-b+1} \sum_{t=1}^{n-b+1} \mathbb{1} \{ \tau_b V_{n,b,t} \leq x \},$$

$$\hat{F}_{n,b}(x) = \frac{1}{n-b+1} \sum_{t=1}^{n-b+1} \mathbb{1} \{ \tau_b \hat{V}_{n,b,t} \leq x \}.$$

For  $\gamma_2 \in (0, 1)$  the quantities  $q(\gamma_2)$ ,  $q_{n,b}(\gamma_2)$  and  $\hat{q}_{n,b}(\gamma_2)$  denote respectively the  $\gamma_2$ -quantiles with respect the distributions  $F$ ,  $F_{n,b}$  and  $\hat{F}_{n,b}$  respectively. We adopt the usual definition that  $q(\gamma_2) = \inf \{x : F(x) \geq \gamma_2\}$ . Lemma 4 in the Appendix states the same consistency for the quantiles.

As noted previously, it is practically impossible to estimate  $s(t)$  given the massive nature of  $n$ . Therefore, a second variant is to reduce the number of subsamples by introducing a random block selection with  $s(t)$  estimated block-wise on subsamples of length  $b$ . Let  $I_i$ ,  $i = 1, \dots, K$  be random variables indicating the initial point of every block of length  $b$ . We draw the sequence  $\{I_i\}_{i=1}^K$ , with/without replacement, from the set  $I = \{1, 2, \dots, n-b+1\}$ . The empirical distribution function of the subsampling variances of  $\hat{\varepsilon}_t$  over the random blocks is

$$\tilde{G}_{n,b}(x) = \frac{1}{K} \sum_{i=1}^K \mathbb{1} \left\{ \tau_b \left( \hat{V}_{n,b,I_i} - V_n \right) \leq x \right\}.$$

The following result states the consistency of  $\tilde{G}$  in approximating  $G$ .

**Proposition 2.** *Assume **A1**, **A2** with  $5/8 < \gamma_1 \leq 1$ , **A3** and **A4**. Let  $\hat{s}(t)$  be the estimate of  $s(t)$  on a subsample of length  $b$ . Let  $n \rightarrow \infty$ ,  $b \rightarrow \infty$ ,  $b/n \rightarrow 0$ , and  $K \rightarrow \infty$ , then  $\sup_x \left| \tilde{G}_{n,b}(x) - G(x) \right| \xrightarrow{p} 0$ .*

Proof of Proposition 2 is given in the Appendix. In analogy with what we have seen before we also establish consistency for the quantiles based on  $\left\{ \hat{V}_{n,b,I_i} \right\}_{i=1}^K$ . Let define the distribution function

$$\tilde{F}_{n,b}(x) = \frac{1}{K} \sum_{t=1}^K \mathbb{1} \left\{ \tau_b \hat{V}_{n,b,I_t} \leq x \right\},$$

and let  $\tilde{q}_{n,b}(\gamma_2)$  be the  $\gamma_2$ -quantile with respect to  $\tilde{F}$ .

**Corollary 1.** *Assume **A1**, **A2** with  $5/8 < \gamma_1 \leq 1$ , **A3** and **A4**. Let  $\hat{s}(t)$  be the estimate of  $s(t)$  on a subsample of length  $b$ . Let  $n \rightarrow \infty$ ,  $b \rightarrow \infty$ ,  $b/n \rightarrow 0$ , and  $K \rightarrow \infty$ , then  $\tilde{q}_{n,b}(\gamma_2) \xrightarrow{p} q(\gamma_2)$ .*

Proof of Corollary 1 is given in the Appendix.

**Remark 3.** Note that the condition that  $5/8 < \gamma_1 \leq 1$  in **A2** is required to achieve the optimal rate for the estimation of  $s(t)$  subsample-wise. Consistency for the estimation of the distribution, and the quantiles of the RMS power is achieved without any identification of the SRD or LRD regime.

A limitation in the procedure is the fixed nature of the block length  $b$ . The reader could find hard to believe that in practice a fixed  $b$  can produce good results. For instance Figure 1 has been constructed so that there are two blocks of observations of equal size that have tremendously different structures. The question is what would happen if a random block, like the one in the top plot, had been extracted. In principle, one can think about estimating an optimal block size  $b$ , but again we have to accept that the astronomically large nature of  $n$  would take the whole estimation time at Biblical scales. Notwithstanding these limitations, we propose a practical solution that is based on the intimate relation between the block length  $b$  and the optimal global bandwidth parameter  $\hat{h}$ . In fact, if a random block is large enough to contain piece of sounds with different dynamic structures, since the bandwidth across the block is taken fixed, the  $\hat{h}$  needs to become small enough to well fit the curve in the transition between two different dynamic stages. In those situations  $\hat{h}$  will approach the lower bound of  $H$ . What we do in practice is that we start from a given  $b$ , then if  $\hat{h}$  is equal to its lower bound we split the block into halves and we recompute  $\hat{h}$  on one of the two halves chosen at random, and if the new  $\hat{h}$  is still on the boundary we iterate the splitting up to the point when the estimated bandwidth is within  $H$ , or a maximum number  $r_{\max}$  of splits has been reached.

**Remark 4.** The splitting step is a practical solution to avoid estimation of  $b$  and/or the use of local bandwidth in the smoothing step. It can be easily seen that, when splitting happens, the resulting block length depends on  $\hat{h}$  and the consistency results stated previously do not account for it. However, on real world sound waves splitting only happens on a small fraction of blocks for various reasonable values of  $b$ . Consistency theory for the estimated  $b$  is possible but would require theoretical developments too complex to be contained in this paper, whose focus is methodological. The choice of  $b$  still remains a crucial tuning but as we will see in Section 6, this can be done rather easily based on subject matter considerations.

## 5 Dynamic range statistic

The random nature of  $\{\varepsilon_t\}_{t \in \mathbb{Z}}$  allows us to use statistical theory to estimate its distribution. If the SSW catches transient energy variations, then its distribution will highlight important information about the dynamic. The square root of  $\hat{V}_{n,b,I_i}$  is a consistent estimate of the RMS power of  $\varepsilon_t$  over the block starting from  $t = I_i$ . The loudness of the  $\{\varepsilon_t\}_{t \in \mathbb{Z}}$  component over each block can be measured on the dBFS scale taking  $\text{DR}_{n,b,I_i} = -10 \log_{10} \hat{V}_{n,b,I_i}$ . Notice that whenever we take continuous monotone transformations of  $\hat{V}_{n,b,I_i}$ , consistency for the quantities obtained through the subsampling is preserved.

In analogy with DRS (and its variants) we can define a DR measure based on the subsampling distribution of  $\hat{V}_{n,b,I_i}$ . We define the DR measure block-wise as  $\text{DR}_{n,b,I_i} = -10 \log_{10} \hat{V}_{n,b,I_i}$ . For a sound wave scaled onto the interval  $[-1,1]$  this is actually a measure of DR of  $\varepsilon_t$  because it tells us how much the SSW is below the maximum attainable instantaneous power. We propose a measure of DR by taking the median of the subsampling distribution of  $\text{DR}_{n,b,I_i}$ , that is we define what we call “*Median Stochastic DR*” as

$$\text{MeSDR} = \text{med}_K \{ \text{DR}_{n,b,I_i} \quad i = 1, 2, \dots, K \},$$

where  $\text{med}_K\{\cdot\}$  denotes the empirical median over a set of  $K$  observations. For waves scaled onto  $[-1,1]$  it is easy to see that our statistic is expressed in dBFS. If the wave is not scaled onto  $[-1,1]$ , it suffices to add  $20 \log_{10}(\text{maximum absolute observed sample})$ , and this will correct for PCM headroom.

The MeSDR has a nice practical interpretation. Suppose  $\text{MeSDR}=20$ , this means that 50% of the stochastic sound power is at least 10dBFS below the maximum instantaneous power. Hence large values of MeSDR indicates large dynamic swings. There are several advantages of such a measure. The DRS statistic is based on mean values which will be pushed toward the peak power it wants to compare. Contrary to what happens to DRS, the MeSDR is less influenced by the peaks. It is important to notice that here the choice of the median, as centrality statistic, is not because we want to be robust. The choice of a less efficient centrality statistic is due to the fact that the mean would be influenced by the right tail of the power distribution. DR wants to express the discrepancy between the main mass of the power distribution and its tails. Hence centrality statistics that are attracted by the tails of the distribution are not appropriate here. It can be argued that the SSW not only catches transients and nonperiodic smooth components. In fact, it's likely that it fits forms of noise, such as quantization noise and/or electrical noise. This is certainly true, but quantization noise operates at extremely low levels and its power distribution is time-invariant. Moreover, since it is likely that digital operations producing DR compression (compressors, limiters, equalizers, etc.) increase the quantization noise (in theory this is not serially correlated), this would reflect in a decrease of MeSDR, so we should be able to detect DR compression better than classical DRS-like measures.

## 6 Empirical Analysis

### 6.1 Simulated compression

A common way of assessing a statistical procedure is to simulate data from a certain known stochastic process fixed as the reference truth, and then compute Monte Carlo expectations of bias and efficiency measures. The problem here is that writing down a stochastic model capable of reproducing the features of real-world music signal is too complex. Instead of trying to simulate such a complex signal we assess our methods based on artificial controlled experiments on real data. We considered two well recorded songs and we added various degrees of dynamic compression to assess whether our measure is able to highlight differences. A good method for estimating a measure of DR should consistently measure the loss of DR introduced by compressing the dynamic. A dynamic compressor is a function that whenever the original signal exceeds a given power (threshold parameter), the power of the output is scaled down by a certain factor (compression ratio parameter). From the statistical viewpoint this is similar to the well-known Box-Cox transform. Compression reduces the weight of tails of the power distribution, so that the distance between average signal level and peak level is reduced. This increases the perceived loudness, but when applied massively it destroys the music.

In order to achieve a fair comparison we need songs on which little amount of digital



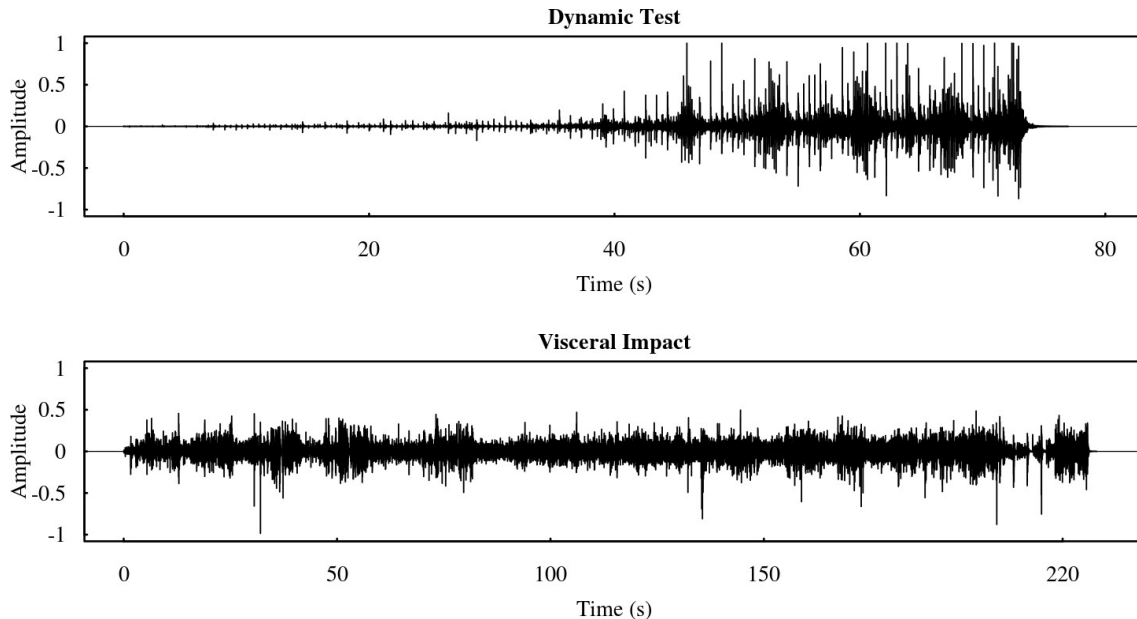


Figure 4: Waveforms of the left channel of the songs titled “*Dynamic Test*” (track no.29), and “*Visceral Impact*” (track no.17) from the audiophile CD “*Ultimate Demonstration Disc: Chesky Records’ Guide to Critical Listening*” (Chesky Record, catalog no. UD95).

processing has been applied. Chesky Records is a small label specialized in audiophile recordings, their “*Ultimate Demonstration Disc: Chesky Records’ Guide to Critical Listening*” (catalog number UD95), is almost a standard among audiophiles as test source for various aspects of hifi reproduction. We consider the left channel of tracks no.29, called “*Dynamic Test*”, and track no.17 called “*Visceral Impact*”. Both waveforms are reported in Figure 4. The “*Dynamic Test*” consists in a drum recorded near-field played with an increasing level. Its sound power is so huge that a voice message warns against play backs at deliberately high volumes, which in fact could cause equipment and hearing damages. Most audiophiles subjectively consider this track as one of the most illustrious example of dynamic recording. The track is roughly one minute long. The “*Visceral Impact*” is actually the song “*Sweet Georgia Brown*” by Monty Alexander and elsewhere published in the Chesky catalog. The song has an energetic groove from the beginning to the end and it’s about three minutes long. Differently from the previous track, this song has a uniform path. This can be clearly seen in Figure 4.

We removed initial and final silence from both tracks, and the final length (in sample units) for “*Dynamic Test*” is  $n = 2,646,000$ , while  $n = 7,938,000$  for the second song. We then applied compression on both waves. We applied compression ratios from 1.5 to 5 with 0.5 increments, and in each case we compressed at threshold levels equal to -12dBFS and -24dBFS. With a threshold of -12dBFS and a compression ratio of 1.5, whenever the signal power is above -12dBFS, the compressor reduces the signal level to  $2/3$  so that the input power is  $1.5 \times (\text{output power})$ . All this has been performed using SoX, an high quality audio digital processing software freely available, with all other tuning parameters set at default values. For each wave we generated sixteen cases additional to the original wave. For each compressed version of the two waves we have computed our MeSDR statistics. In Figure 5 we report our results.

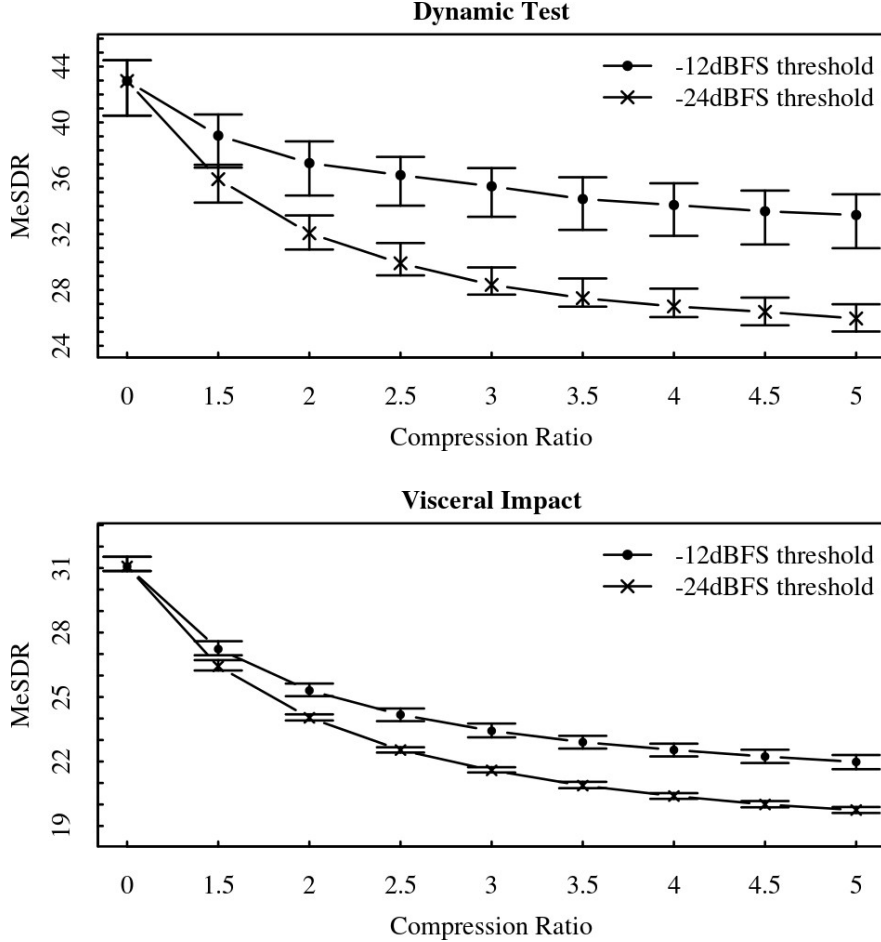


Figure 5: MeSDR statistics with 95%-confidence bands for the simulated compression experiment.

The subsampling has been run with several sets of input parameters to assess its stability. The results in Figure 5 are obtained with  $K = 500$  for both songs, while  $b = 2205$  (which means 50ms) for “*Dynamic Test*”, and  $b = 3528$  (which means 80ms) for “*Visceral Impact*”. A larger  $b$  for larger  $n$  obeys to the theoretical requirements that  $b/n \rightarrow 0$  as  $n$  and  $b$  grow to  $\infty$ . We also tried with larger values of  $b$  for both tracks but results did not change overall. Notice that while the theory is developed for fixed  $b$ , in practice we allow for smaller values of  $b$  by the splitting step (see Remark 4). In these cases the splitting never happened on more than 5% of subsamples. A 50ms block length for the second track would not have changed the results either.  $K = 1000$  would not add too much to what we can find with  $K = 500$ . In Figure 5 we report a plot of MeSDR statistics with 95%-confidence bands based on Corollary 1. Notice that we could have approximated the confidence bands for MeSDR with more precision by using the fact that  $\tau_n(V_n - \sigma_\varepsilon^2) \xrightarrow{d} G(\cdot)$ , where  $G(\cdot)$  is a Normal distribution under both SRD and LRD with  $5/8 < \gamma_1 \leq 1$  (see Remark 5). However, this requires further theoretical developments not justified by the small gain in precision. In a comparison like this, one can choose to fix the seeds for all cases so that MeSDR is computed over the same subsamples in all cases. However this would not allow to assess the stability of the procedure against subsampling induced variance. The results presented here are obtained with different seeds for each case, but fixed seed has

been tested and it did not change the main results. The constant  $M$  is fixed according to Proposition 1, i.e.  $M = \lfloor \sqrt{n\hat{h}} \rfloor$ .

First of all we notice that in all cases MeSDR can reproduce the somehow theoretical behaviour of DR vs compression ratios. If we had an input signal with constant unit RMS power, as the compression ratio increases DR should decrease at the speed of  $\log_{10}(1/\text{compression ratio})$  for any threshold value. Of course, when the RMS power is not constant this is not true anymore but we expect a behaviour similar to the curve  $y = \log_{10}(1/x)$  for  $x > 0$ . At both threshold levels for both songs the MeSDR does a remarkable discrimination between compression levels. For a given positive compression level, none of the confidence bands for the -12dBFS threshold overlaps with the confidence bands for the -24dBFS case. For both songs the confidence bands are longer for the -12dBFS case, and on average the “Dynamic Test” reports longer bands. This is expected, and it is a consistent behavior. In fact, moving the threshold from -12dBFS to -24dBFS will increase the proportion of samples affected by compression, so that the variations of MeSDR will be reduced. Moreover we also expect that if the dynamic of a song doesn’t have a sort of uniform path, as in the case of the “Dynamic Test”, the variability of the MeSDR will be larger. Summarizing, not only the level of MeSDR, but also its spread reveals important information on the DR. The example above shows how MeSDR is able to detect consistently even small amount of compression.

## 6.2 Comparing different masterings

There are a number small record labels that gained success issuing remastered versions of famous albums. Some of this reissues are now out of catalogue and are traded at incredible prices on the second hand market. That means that music lovers actually price the value of the recording quality. On the other hand majors keep issuing new remastered versions promising miracles, they often claim the use of new super technologies termed with spectacular names. But many music lovers are very critical because human ears perceive dynamic at an high level of resolution. In this section we measure the DR of three different digital masterings of the song “In the Flesh?” from “*The Wall*” album by Pink Floyd. The album is considered one of the best rock recording of all times and “In the Flesh?” is a champion in dynamic, especially in the beginning (as reported in Figure 1) and at the end. We analysed three different masters: the MFSL by Mobile Fidelity Sound Lab (catalog UDCD 2-537, issued in 1990); EMI94 by EMI Records Ltd (catalog 8312432, issued in 1994); EMI01 produced by EMI Music Distribution (catalog 679182, issued in 2001). There are much more remasters of the album not considered here. The EMI01 has been marketed as a remaster with superior sound obtained with state of the art technology. The MFSL has been worked out by a company specialized in classic album remasters. The first impression is that the MFSL sounds softer than the EMI versions. However, there are Pink Floyd fans arguing that the MFSL sounds more dynamic, and overall is better than anything else. Also the difference between the EMI94 and EMI01 is often discussed on web forums with fans arguing that EMI01 did not improved upon EMI94 as advertised.

We measured the MeSDR of the three tracks and compared the results. Since the large correlation between the two channels, we only measured the channel with the largest peak, that is the left one. The three waves have been time-aligned, and the initial and final si-

Table 1: DR statistics for the left channel of “*In the Flesh?*” from “*The Wall*” album by Pink Floyd. “Lower” and “Upper” columns are limits of the 95%-confidence interval.

Seed Number	Version	MeSDR	Lower	Upper
Equal	MFSL	29.30	27.852	31.175
	EMI94	25.53	24.732	26.550
	EMI01	25.38	24.654	26.270
Unequal	MFSL	29.25	27.763	31.187
	EMI94	25.38	24.625	26.453
	EMI01	25.49	24.497	26.288

lence has been trimmed. The MeSDR has been computed with a block length of  $b = 2205$  (that is 50ms), and  $K = 500$ . We computed the MeSDR both with equal and unequal seeds across the three waves to test for subsampling induced variability when  $K$  is on the low side. Results are summarized in Table 1. First notice the seed changes the MeSDR only slightly. Increasing the value of  $K$  to 1000 would make this difference even smaller. The second thing to notice is that MeSDR reports almost no difference between EMI94 and EMI01. Moreover the MFSL reports longer 95% confidence bands and these do not overlap with those of the other masterings. In a way the figure provided by the MeSDR is consistent with most subjective opinions that the MFSL, while sounding softer, has more dynamic textures.

A further question is whether there are statistically significant differences between the sound power distributions of the tracks. Our subsampling approach can indeed answer to this kind of question by hypothesis testing. If the autocorrelations of  $\varepsilon_t$  go to zero at a proper rate, one can take the loudness measurements  $\{\text{DR}_{n,b,I_i} \quad i = 1, 2, \dots, K\}$  as almost asymptotically independent and then apply some standard tests for location shift. This is straightforward for the SRD case. Under LRD assumption asymptotic independence is less intuitive but can be argued just following the arguments of the proof of Lemma 2 in the Appendix. One can study an ad-hoc test for this problem. In this paper we simply apply an handy simple test like the Mann-Whitney. Based on the setup with unequal seeds, we applied the Mann-Whitney test for the null hypothesis that the DR measurements of MFSL and EMI94 are not location-shifted, against the alternative that MFSL is right shifted with respect to EMI94. The resulting p-value  $< 2.2 \times 10^{-16}$  suggests to reject the null at any sensible confidence level, and this confirms that MFSL sounds more dynamic compared to EMI94. Comparison between MFSL and EMI01 leads to a similar result. We also tested the null hypothesis DR measurements of EMI94 and EMI01 are not location-shifted, against the alternative that there is some shift different from zero. The resulting p-value=0.6797 suggests to not reject the null at any standard confidence level. The latter confirms the figure suggested by MeSDR that is there is no significant overall dynamic difference between the two masterings.

## 7 Concluding Remarks

Starting from the DR problem we exploited a methodology to estimate the variance distribution of a time series produced by a stochastic process additive to a smooth function of time. The general set of assumptions on the error term makes the proposed model flexible and general enough to be applied under various situations not explored in this paper. The smoothing and the subsampling theory is developed for fixed global bandwidth and fixed subsample size. Optimal block size would be useful, but because of the typical large  $n$ , we proposed a splitting strategy that allows to vary the block lengths starting from a maximum. The study of the theoretical properties of the splitting will be the subject of another paper. We constructed a DR statistic that allows inference. Our proposal is to capture the DR concept based on a stochastic component. This has two main advantages: (i) technically speaking it allows to handle the sampling variations by means of inferential procedures; (ii) since power variations are about sharp changes in the energy levels, it is likely that these changes will affect the stochastic part of (5) more than the smooth component. In controlled experiment our DR statistic has been able to highlight consistently dynamic range compressions. Moreover we provided an example where the MeSDR statistic is able to reconstruct differences perceived subjectively on real music signals.

## Appendix: proofs

In this section we report the proofs of statements and some useful technical lemmas. First, we state a lemma to evaluate the  $MISE(\hat{s}; h)$ .

**Lemma 1.** *Assume [A1](#), [A2](#) and [A3](#). For  $t \in I_h = (h, 1 - h)$*

$$MISE(\hat{s}; h) = \frac{h^4 R(s'')}{4} d_K + \sigma_\varepsilon^2 \frac{N_K}{nh} + 2\sigma_\varepsilon^2 N_K \frac{S_\rho^*}{\Lambda_n h} + o\left(\frac{1}{\Lambda_n h} + h^4\right),$$

where  $\hat{s}$  is the kernel estimator in [\(6\)](#),  $R(s'') = \int_{I_h} [s''(t)]^2 dt$ ,  $d_K = \int u^2 K(u) du$ ,  $N_K = \int K^2(u) du$ ,  $\sigma_\varepsilon^2 = E[\varepsilon_t^2]$ ,  $\Lambda_n$  is defined in [\(7\)](#) and

$$S_\rho^* := \begin{cases} \lim_{n \rightarrow \infty} \sum_{j=1}^n \rho(j) & \text{if [A2-SRD](#) holds} \\ \lim_{n \rightarrow \infty} \frac{1}{\log n} \sum_{j=1}^n \rho(j) & \text{if [A2-LRD](#) holds with } \gamma_1 = 1 \\ \lim_{n \rightarrow \infty} \frac{1}{n^{1-\gamma_1}} \sum_{j=1}^n \rho(j) & \text{if [A2-LRD](#) holds with } 1/5 < \gamma_1 < 1. \end{cases} \quad (11)$$

*Proof.* By [A3](#) it follows that conditions A-C of [Altman \(1990\)](#) are satisfied. Now, let

$$\rho_n(j) := \begin{cases} \rho(j) & \text{if [A2-SRD](#) holds} \\ \frac{1}{\log n} \rho(j) & \text{if [A2-LRD](#) holds with } \gamma_1 = 1 \\ \frac{1}{n^{1-\gamma_1}} \rho(j) & \text{if [A2-LRD](#) holds with } 1/5 < \gamma_1 < 1. \end{cases}$$

For the cases SRD and LRD with  $\gamma_1 = 1$  the conditions D and E of [Altman \(1990\)](#) are still satisfied with  $\rho_n(j)$ . Following the same arguments as in the proof of [Theorem 1](#) of [Altman \(1990\)](#) the result follows. Finally, in the last case,  $\rho_n(j)$  satisfies condition D but not condition E of [Altman \(1990\)](#). So, we have

$$\sum_{j=1}^n j \rho_n(j) = O(n).$$

Therefore, using [Lemma A.4](#) in [Altman \(1990\)](#), it follows that

$$\text{Var}[\hat{s}] = \sigma_\varepsilon^2 \frac{N_K}{nh} + 2\sigma_\varepsilon^2 N_K \frac{S_\rho^*}{\Lambda_n h} + o\left(\frac{1}{\Lambda_n h}\right).$$

The latter completes the proof.  $\square$

Note that [Lemma 1](#) gives a similar formula to [\(2.8\)](#) in [Theorem 2.1](#) of [Hall et al. \(1995\)](#). However, differently from [Hall et al. \(1995\)](#) our approach does not need to introduce an additional parameter to capture SRD and LRD. Also notice that taking  $h \in H$  as in [A3](#), implies that  $MISE(\hat{s}; h) = O\left(\Lambda_n^{-4/5}\right)$ , which means that the kernel estimator achieves the global optimal rate.

**Proof of Proposition 1.** [Lemma 1](#) holds under [A1](#), [A2](#) and [A3](#). Let  $\hat{\gamma}(j) = \frac{1}{n} \sum_{t=1}^{n-j} \hat{\varepsilon}_t \hat{\varepsilon}_{t+j}$  be the estimator of the autocovariance  $\gamma(j)$  with  $j = 0, 1, \dots$ . By [A3](#)  $r_n = \frac{1}{\Lambda_n h} + h^4 =$



$\Lambda_n^{-4/5}$ , and by Markov inequality

$$\frac{1}{n} \sum_{i=1}^n (s(i/n) - \hat{s}(i/n))^2 \xrightarrow{P} \text{MISE}(\hat{s}; h) + o(r_n) \quad (12)$$

Rewrite  $\hat{\gamma}(j)$  as

$$\begin{aligned} \hat{\gamma}(j) &= \frac{1}{n} \sum_{i=1}^{n-j} (s(i/n) - \hat{s}(i/n)) (s((i+j)/n) - \hat{s}((i+j)/n)) + \\ &+ \frac{1}{n} \sum_{i=1}^{n-j} (s((i+j)/n) - \hat{s}((i+j)/n)) \varepsilon_i + \\ &+ \frac{1}{n} \sum_{i=1}^{n-j} (s(i/n) - \hat{s}(i/n)) \varepsilon_{i+j} + \frac{1}{n} \sum_{i=1}^{n-j} \varepsilon_i \varepsilon_{i+j} = \text{I} + \text{II} + \text{III} + \text{IV}. \end{aligned} \quad (13)$$

By (12) and Schwartz inequality it results that term I =  $O_p(r_n)$  in  $\hat{\gamma}(j)$ . Consider term III in (13). Since  $\hat{s}(t) = s(t)(1 + O_p(r_n^{1/2}))$ , it is sufficient to investigate the behaviour of

$$\frac{1}{n} \sum_{i=1}^{n-j} s(i/n) \varepsilon_{i+j}.$$

$\sum_j^n \rho(j) = O(\log n)$  under LRD with  $\gamma_1 = 1$ , and  $\sum_j^n \rho(j) = O(n^{1-\gamma_1})$  under LRD with  $1/5 < \gamma_1 < 1$ . By **A1**, and applying Chebishev inequality, it happens that III =  $O_p(\Lambda_n^{-1/2})$ . Based on similar arguments one has that term II =  $O_p(\Lambda_n^{-1/2})$ . Now consider last term of (13), and notice that it is the series of products of autocovariances. Theorem 3 in **Hosking (1996)** is used to conclude that the series is convergent under SRD and LRD with  $1/2 < \gamma_1 \leq 1$ , while it is divergent under LRD with  $1/5 < \gamma_1 \leq 1/2$ . Based on this, direct application of Chebishev inequality to term IV implies that IV =  $O_p(\Lambda_n^{-1/2})$ . Then  $\hat{\gamma}(j) = \gamma(j) + O_p(r_n) + O_p(\Lambda_n^{-1/2}) + O_p(j/n)$ , where the  $O_p(j/n)$  is due to the bias of  $\hat{\gamma}(j)$ . This means that  $\hat{\rho}(j) = \rho(j) + O_p(r_n) + O_p(\Lambda_n^{-1/2}) + O_p(j/n)$ . Since  $K(\cdot)$  is bounded then one can write

$$\frac{1}{nh} \sum_{j=-M}^M K\left(\frac{j}{nh}\right) \hat{\rho}(j) = \frac{1}{nh} \sum_{j=-M}^M K\left(\frac{j}{nh}\right) \rho(j) + \frac{M}{nh} O_p(r_n) + \frac{M}{nh} O_p(\Lambda_n^{-1/2}) + \frac{M^2}{n} O_p\left(\frac{1}{nh}\right).$$

Using **A4** and  $h = O(\Lambda_n^{-1/5})$ , **A3** implies that

$$\frac{1}{nh} \sum_{j=-M}^M K\left(\frac{j}{nh}\right) \hat{\rho}(j) = \frac{1}{nh} \sum_{j=-M}^M K\left(\frac{j}{nh}\right) \rho(j) + o_p(r_n). \quad (14)$$

Now take  $(nh/2)_* = \text{round}(nh/2)$  and write

$$Q_1 = \left| \frac{1}{nh} \sum_{j=-nh/2}^{(nh/2)_*} K\left(\frac{j}{nh}\right) \rho(j) - \frac{1}{nh} \sum_{j=-M}^M K\left(\frac{j}{nh}\right) \hat{\rho}(j) \right|.$$

By (14), it follows that

$$Q_1 = \left| \frac{2}{nh} \sum_{j=-M+1}^{(nh/2)^*} K\left(\frac{j}{nh}\right) \rho(j) \right| + o_p(r_n).$$

By [A2](#), [A3](#) and [A4](#),

$$\frac{1}{nh} \sum_{j=-M+1}^{(nh/2)^*} K\left(\frac{j}{nh}\right) \rho(j) \sim \rho(nh - M) = o(r_n),$$

which implies that  $Q_1 = o_p(r_n)$ . Notice that the first term in  $Q_1$  is the analog of expression (22) in [Altman \(1990\)](#). Therefore,  $CV(h)$  can now be written as

$$\begin{aligned} CV(h) &= \left[ 1 - \frac{1}{nh} \sum_{j=-M}^M K\left(\frac{j}{nh}\right) \hat{\rho}(j) \right]^{-2} \frac{1}{n} \sum_{i=1}^n \hat{\varepsilon}_i^2 \\ &= \left[ 1 - \frac{1}{nh} \sum_{j=-nh/2}^{(nh/2)^*} K\left(\frac{j}{nh}\right) \rho(j) \right]^{-2} \frac{1}{n} \sum_{i=1}^n \hat{\varepsilon}_i^2 + o_p(r_n). \end{aligned}$$

Apply the classical bias correction, and based on (14) in [Altman \(1990\)](#), we have that

$$CV(h) = \frac{1}{n} \sum_{t=1}^n \varepsilon_t^2 + \text{MISE}(\hat{s}; h) + o_p(r_n),$$

using the same arguments as in the proof of Theorem 1 in [Chu and Marron \(1991\)](#).  $\text{MISE}(\hat{s}; h) = O(r_n)$  by Lemma 1. Hence,  $\hat{h}$  is equal to  $h^*$  asymptotically in probability.  $\square$

The following Remark and the subsequent Lemmas are needed to show Proposition 2 and Corollary 1.

**Remark 5.** By [A2](#) it can be shown that  $\tau_n(V_n - \sigma_\varepsilon^2) \xrightarrow{d} G(\cdot)$ , where  $\sigma_\varepsilon^2 = E[\varepsilon_t^2]$ . Under [A2-SRD](#),  $G(\cdot)$  is a Normal distribution.  $G(\cdot)$  is still a Normal distribution under [A2-LRD](#) with  $1/2 < \gamma_1 \leq 1$ , which follows from Theorem 4 of [Hosking \(1996\)](#). The same Theorem implies that  $G(\cdot)$  is Normal under [A2-LRD](#) with  $\gamma_1 = 1/2$  when  $a_t$  is normally distributed. Moreover,  $G(\cdot)$  is not Normal under [A2-LRD](#) with  $1/5 < \gamma_1 < 1/2$ .

**Lemma 2.** Assume [A2](#), and assume  $a_t \sim N(0, \sigma_a^2)$  for every  $t \in \mathbb{Z}$  whenever  $1/5 < \gamma_1 \leq 1/2$ . Then  $n \rightarrow \infty$ ,  $b \rightarrow \infty$  and  $b/n \rightarrow 0$  implies  $\sup_x |G_{n,b}(x) - G(x)| \xrightarrow{p} 0$ , and  $q_{n,b}(\gamma_2) \xrightarrow{p} q(\gamma_2)$  for all  $\gamma_2 \in (0, 1)$ .

*Proof.* Under [A2-SRD](#), Theorems 4.1 and 5.1 of [Politis et al. \(2001\)](#) hold and the results follow. The rest of the proof deals with the LRD case. Since  $G(x)$  is continuous (see [Hosking, 1996](#)), we follow proof of Theorem 4 of [Jach et al. \(2012\)](#). Fix  $G_{n,b}^0(x) = \frac{1}{N} \sum_{i=1}^N \mathbb{1} \{ \tau_b(V_{n,b,i} - \sigma_\varepsilon^2) \leq x \}$  with  $N = n - b + 1$ . It is sufficient to show that  $\text{Var}[G_{n,b}^0(x)] \rightarrow 0$  as  $n \rightarrow \infty$ . Apply Theorem 2 in [Hosking \(1996\)](#) to conclude that  $\tau_n(V_n - \sigma_\varepsilon^2)$  has the same distribution as  $\tau_n(V_n^1)$ , where  $V_n^1 = \frac{1}{n} \sum_{i=1}^n (\varepsilon_i^2 - \sigma_\varepsilon^2)$ .

Therefore, we have to show that  $\text{Var}[G_{n,b}^1(x)] \rightarrow 0$  as  $n \rightarrow \infty$ , where

$$G_{n,b}^1(x) = \frac{1}{N} \sum_{i=1}^N \mathbb{1}\{\tau_b V_{n,b,i}^1 \leq x\} \quad \text{with} \quad V_{n,b,i}^1 = \frac{1}{b} \sum_{j=1}^b (\varepsilon_{j+i-1}^2 - \sigma_\varepsilon^2).$$

Using the stationarity of  $\{\varepsilon_t\}_{t \in \mathbb{Z}}$ , it follows that  $\text{Var}[G_{n,b}^1(x)] = \text{E}[(G_{n,b}^1(x) - G_b^1(x))^2]$ , where  $G_b^1(x) = P(\tau_b V_b^1 \leq x)$ . Based the same arguments as in the proof of Theorem 2.2 of [Hall et al. \(1998\)](#) with  $q = 2$ , we can write

$$\text{Var}[G_{n,b}^1(x)] \leq \frac{2b+1}{N} G_b^1(x) + \frac{2}{N} \sum_{i=b+1}^{N-1} \left| P(\tau_b V_{n,b,1}^1 \leq x, \tau_b V_{n,b,i+1}^1 \leq x) - [G_b^1(x)]^2 \right|. \quad (15)$$

Consider

$$\text{Cov}[\tau_b V_{n,b,1}^1, \tau_b V_{n,b,N}^1] = \frac{\tau_b^2}{b^2} \left( \sum_{i=1}^b (\varepsilon_i^2 - \sigma_\varepsilon^2) \cdot \sum_{i=1}^b (\varepsilon_{i+N-1}^2 - \sigma_\varepsilon^2) \right).$$

After some algebra, we obtain

$$\text{Cov}[\tau_b V_{n,b,1}^1, \tau_b V_{n,b,N}^1] = \frac{\tau_b^2}{b} \sum_{k=-(b-1)}^{b-1} \left( 1 - \frac{|k|}{b} \right) \phi_2(k+N), \quad (16)$$

where for  $k = 1, 2, \dots$ ,  $\phi_2(k)$  are the autocovariances of  $\{\varepsilon_t\}_{t \in \mathbb{Z}}$ . For  $k \rightarrow \infty$ , **A2**-LRD with  $1/5 < \gamma_1 \leq 1$  implies that  $\phi_2(k) = O(k^{-2\gamma_1})$  by Theorem 3 of [Hosking \(1996\)](#). Take (16) and note that

$$|\text{Cov}[\tau_b V_{n,b,1}^1, \tau_b V_{n,b,N}^1]| \leq \frac{\tau_b^2}{b} \sum_{k=-(b-1)}^{b-1} |\phi_2(k+N)| \leq \frac{\tau_b^2}{b} \left( \frac{1}{N-b+1} \right)^{2\gamma_1} C_b,$$

where

$$C_b := \begin{cases} O(1) & 1/2 < \gamma_1 \leq 1, \\ O(\log b) & \gamma_1 = 1/2, \\ O(b^{1-2\gamma_1}) & 1/5 < \gamma_1 < 1/2. \end{cases}$$

The latter implies that for  $n \rightarrow \infty$ , (16) converges to zero. Therefore,  $\tau_b V_{n,b,1}^1$  and  $\tau_b V_{n,b,N}^1$  are asymptotically independent. The latter can be argued based on asymptotic normality when  $1/2 < \gamma_1 \leq 1$ . For the case  $1/5 < \gamma_1 \leq 1/2$  the asymptotic independence can be obtained based on the same arguments as in the proof of Theorem 2.2 of [Hall et al. \(1998\)](#). Thus, right hand side of (15) converges to zero as  $n \rightarrow \infty$  by Cesaro Theorem. The latter shows that  $\sup_x |G_{n,b}(x) - G(x)| \xrightarrow{P} 0$ .

Following the same arguments as in Theorem 5.1 of [Politis et al. \(2001\)](#), and by using the first part of this proof one shows that  $q_{n,b}(\gamma_2) \xrightarrow{P} q(\gamma_2)$ . The latter completes the proof.  $\square$

**Lemma 3.** Assume **A1**, **A2**, **A3** and **A4**. Assume that  $a_t$  is normally distributed whenever  $1/5 < \gamma_1 \leq 1/2$ . Let  $\hat{s}(t)$  be the estimate of  $s(t)$  computed on the entire sample (of length  $n$ ). Then  $n \rightarrow \infty$  and  $b = o(n^{4/5})$  implies  $\sup_x |\hat{G}_{n,b}(x) - G(x)| \xrightarrow{P} 0$ .

*Proof.* Denote  $r_n = \frac{1}{\Lambda_n h} + h^4$ . By Lemma 1 and A3,  $r_n = \Lambda_n^{-\frac{4}{5}}$ .  $\hat{s}(t)$  is computed on the whole time series, and by (12)

$$\frac{1}{b} \sum_{t=1}^b (\hat{\varepsilon}_t - \varepsilon_t)^2 = O_p(r_n).$$

$\tau_b r_n \rightarrow 0$  as  $n \rightarrow \infty$ , and it follows that  $\tau_b (\hat{V}_{n,b,t} - V_{n,b,t}) \xrightarrow{P} 0$ . Therefore  $\tau_b (\hat{V}_{n,b,t} - V_n)$  has the same asymptotic distribution as  $\tau_b (V_{n,b,t} - V_n)$ . Denote  $Z_{1t} = \tau_b (V_{n,b,t} - V_n)$  and  $Z_{2t} = \tau_b (\hat{V}_{n,b,t} - V_{n,b,t})$ , so that

$$\hat{G}_{n,b}(x) = \frac{1}{n-b+1} \sum_{t=1}^{n-b+1} \mathbb{1}\{Z_{1t} + Z_{2t} \leq x\}.$$

By the same arguments used for the proof of Slutsky theorem, the previous equation can be written as

$$\sup_x \left| \hat{G}_{n,b}(x) - G(x) \right| \leq \sup_x |G_{n,b}(x \pm \xi_1) - G(x)| + \frac{1}{n-b+1} \sum_{t=1}^{n-b+1} \mathbb{1}\{|Z_{2t}| > \xi_2\},$$

for any positive constants  $\xi_1$  and  $\xi_2$ . Since  $G(x)$  is continuous at any  $x$  (see Remark 5), then  $\sup_x |G_{n,b}(x) - G(x)| \xrightarrow{P} 0$  by Lemma 2. Moreover,  $Z_{2t} \xrightarrow{P} 0$ , for all  $t$  and thus

$$\frac{1}{n-b+1} \sum_{t=1}^{n-b+1} \mathbb{1}\{|Z_{2t}| > \xi_2\} \xrightarrow{P} 0,$$

for all  $\xi_2 > 0$ , which proves the result.  $\square$

**Lemma 4.** Assume A1, A2, A3 and A4. Assume that  $a_t$  is normally distributed whenever  $1/5 < \gamma_1 \leq 1/2$ . Let  $\hat{s}(t)$  be the estimate of  $s(t)$  computed on the entire sample (of length  $n$ ). Then  $n \rightarrow \infty$  and  $b = o(n^{4/5})$  implies  $\hat{q}_{n,b}(\gamma_2) \xrightarrow{P} q(\gamma_2)$  for any  $\gamma_2 \in (0, 1)$ .

*Proof.* Using the same arguments as in Lemma 3 we have that  $\hat{F}_{n,b}(x) - F_{n,b}(x) = o_p(1)$ . By the continuity of  $F(x)$  at all  $x$  we have that  $q_{n,b}(\gamma_2) \xrightarrow{P} q(\gamma_2)$  by Lemma 2. Therefore  $\hat{q}_{n,b}(\gamma_2) \xrightarrow{P} q(\gamma_2)$ .  $\square$

Note that assumption  $b = o(n^{4/5})$  is need to deal with A2-LRD, however for A2-SRD only we would only need  $b = o(n)$ .

**Proof of Proposition 2.** Let  $P^*(X)$  and  $E^*(X)$  be the conditional probability and the conditional expectation of a random variable  $X$  with respect to a set  $\chi = \{Y_1, \dots, Y_n\}$ . Let  $\hat{G}_{n,b}^b(x)$  be the same as  $\hat{G}_{n,b}(x)$ , but now  $\hat{s}(t)$  is estimated on each subsample of length  $b$ . Then,

$$\frac{1}{b} \sum_{i=1}^b (\hat{\varepsilon}_i - \varepsilon_i)^2 \xrightarrow{P} \text{MISE}(\hat{s}; h) = O_p\left(\Lambda_b^{-4/5}\right),$$

using Lemma 1 as in the proof of Lemma 3.  $\tau_b \Lambda_b^{-4/5} \rightarrow 0$  when  $5/8 < \gamma_1 \leq 1$  in assumption A2. So, as in the proof of Lemma 3, it follows that

$$\sup_x \left| \hat{G}_{n,b}^b(x) - G(x) \right| \xrightarrow{P} 0,$$

since  $G(x)$  is continuous for all  $x$  (see Remark 5). Let  $Z_i(x) = \mathbb{1} \left\{ \tau_b \left( \hat{V}_{n,b,i} - V_n \right) \leq x \right\}$  and  $Z_i^*(x) = \mathbb{1} \left\{ \tau_b \left( \hat{V}_{n,b,I_i} - V_n \right) \leq x \right\}$ .  $I_i$  is a random variable from  $I = \{1, 2, \dots, n - b + 1\}$ . Then,  $P(Z_i^*(x) = Z_i(x)) = \frac{1}{n-b+1}$  for all  $i$  and  $x$ . Then  $\tilde{G}_{n,b}(x) = \frac{1}{K} \sum_{i=1}^K Z_i^*(x)$  and

$$E^* \left[ \tilde{G}_{n,b}(x) \right] = \frac{1}{n-b+1} \sum_{t=1}^{n-b+1} Z_t(x) = \hat{G}_{n,b}^b(x) \xrightarrow{P} G(x).$$

Application of Corollary 2.1 in Politis and Romano (1994) leads to

$$\sup_x \left| \tilde{G}_{n,b}(x) - \hat{G}_{n,b}^b(x) \right| \xrightarrow{\text{as}} 0,$$

which proves the statement. □

**Proof of Corollary 1.** The results follows from the proof of Lemma 4 by replacing Lemma 3 with Proposition 2. □

## References

- Altman, N. S. (1990). Kernel smoothing of data with correlated errors. *Journal of the American Statistical Association* 85(411), 749–759.
- Altman, N. S. (1993). Estimating error correlation in nonparametric regression. *Statistics & probability letters* 18(3), 213–218.
- Ballou, G. (2005). *Handbook for Sound Engineers*. Focal Press.
- Bennett, W. R. (1948). Spectra of quantized signals. *Bell Syst. Tech. J* 27(3), 446–472.
- Benson, D. (2006, 12). *Music: A Mathematical Offering* (1 ed.). Cambridge University Press.
- Beran, J. (2004a). Music-chaos, fractals, and information. *Chance* 17(4), 7–16.
- Beran, J. (2004b). *Statistics in musicology*, Volume 12. Boca Raton, Fla: Chapman & Hall/CRC.
- Boley, J., M. Lester, and C. Danner (2010). Measuring dynamics: Comparing and contrasting algorithms for the computation of dynamic range. In *Proceedings of the AES 129th Convention, San Francisco*.
- Brillinger, D. R. and R. A. Irizarry (1998). An investigation of the second-and higher-order spectra of music. *Signal Processing* 65(2), 161–179.

- Chu, C. K. and J. S. Marron (1991). Comparison of two bandwidth selectors with dependent errors. *The Annals of Statistics* 19(4), 1906–1918.
- Crocker, M. J. (1998). *Handbook of Acoustics*. Wiley-Interscience.
- Francisco-Fernández, M., J. Opsomer, and J. M. Vilar-Fernández (2004). Plug-in bandwidth selector for local polynomial regression estimator with correlated errors. *Journal of Nonparametric Statistics* 16(1-2), 127–151.
- Hall, P., B. Y. Jing, and S. N. Lahiri (1998). On the sampling window method for long-range dependent data. *Statistica Sinica* 8, 1189–1204.
- Hall, P., S. N. Lahiri, and J. Polzehl (1995). On bandwidth choice in nonparametric regression with both short- and long-range dependent errors. *The Annals of Statistics* 23(6), 1921–1936.
- Hart, J. D. (1991). Kernel regression estimation with time series errors. *Journal of the Royal Statistical Society. Series B (Methodological)*, 173–187.
- Hosking, J. R. M. (1996). Asymptotic distributions of the sample mean, autocovariances, and autocorrelations of long-memory time series. *Journal of Econometrics* 73, 261–284.
- Irizarry, R. A. (2001). Local harmonic estimation in musical sound signals. *Journal of the American Statistical Association* 96(454), 357–367.
- Jach, A., T. McElroy, and D. N. Politis (2012). Subsampling inference for the mean of heavy-tailed long-memory time series. *Journal of Time Series Analysis* 33, 96–111.
- Katz, B. (2007). *Mastering audio: the art and the science*. Focal Press.
- Perez-Alcazar, P. R. and A. Santos (2002). Relationship between sampling rate and quantization noise. In *14th International Conference on Digital Signal Processing*, Volume 2, pp. 807–810. IEEE.
- Politis, D. N. and J. P. Romano (1994). Large sample confidence regions based on subsamples under minimal assumptions. *The Annals of Statistics* 22(4), 2031–2050.
- Politis, D. N., J. P. Romano, and M. Wolf (2001). On the asymptotic theory of subsampling. *Statistica Sinica* 11(4), 1105–1124.
- Priestley, M. B. and M. T. Chao (1972). Nonparametric function fitting. *Journal of the Royal Statistical Society* 34, 385–392.
- Risset, J. C. and M. V. Mathews (1969). Analysis of musical-instrument tones. *Physics today* 22, 23.
- Vickers, E. (2010). The loudness war: Background, speculation and recommendations. In *Proceedings of the AES 129th Convention, San Francisco, CA*, pp. 4–7.
- von Helmholtz, H. (1885). *On the sensations of tone (English translation AJ Ellis)*. New York: Dover.
- Voss, R. F. and J. Clarke (1975). “1/f noise” in music and speech. *Nature* 258, 317–318.
- Voss, R. F. and J. Clarke (1978). “1/f noise” in music: Music from 1/f noise. *The Journal of the Acoustical Society of America* 63, 258.



Xia, Y. and W. Li (2002). Asymptotic behavior of bandwidth selected by the cross-validation method for local polynomial fitting. *Journal of multivariate analysis* 83(2), 265–287.